Chinese Science Bulletin 2006 Vol. 51 No. 8 977—986

DOI: 10.1007/s11434-006-0977-8

Remote sensing of spatial patterns of urban renewal using linear spectral mixture analysis: A case of central urban area of Shanghai (1997－2000)

YUE Wenze[1], XU Jianhua[2], WU Jiawei[2] & XU Lihua[3]

1. College of Southeast Land Management, Zhejiang University, Hangzhou 310029, China;
2. Department of Geography, East China Normal University, Shanghai 200062, China;
3. Zhejiang Forest University, Lin'an 311300, China

Correspondence should be addressed to Xu Jianhua (email: jhxu@geo.ecnu.edu.cn)

Abstract It is very important to integrate remote sensing with urban geography that the spectral mixture analysis technique is applied to urban land cover evolvement and its eco-environmental effect. Urban land cover is mainly composed of complicated artificial materials, which is the key factor to limit the development of the spectral mixture analysis technique. There are two main aspects in which the technique of spectral mixture analysis is applied to urban geography: one is to calculate vegetation fraction; the other is to build quantitative model of the urban impervious surface obtained from the combination between high albedo fraction and low albedo fraction. The technique of spectral mixture analysis is firstly applied to study urban renewal pattern, scale and mode which happened in Shanghai City from 1997 to 2000.

Keywords: linear spectral analysis, endmember, urban renewal, Shanghai.

Spectral Mixture Analysis (SMA) was utilized for calculating land cover fractions within a pixel and involves modeling a mixed spectrum as a combination of spectra for pure land cover types, called endmembers. SMA, whose core is to mine higher scale level information from relatively low scale data, is a hotspot in the field of processing remote sensing data, which can enrich information and improve the efficiency of remote sensing data[1－5]. The linear spectral mixture model bases on the assumption that the mixed spectrum is a linear combination of endmembers. It also assumes that the same type of land cover is of similar spectrum, which can be added up together[6]. There were abundant studies about linear spectral mixture analysis (LSMA) in which the most popular method is based on constrained least-squares and minimum noise fraction (MNF) transformation[1]. For example, Small showed his way to calculate the vegetation fraction by the means of principle component (PC) transformation based on linear mixture model in 2001[4]. And then, in 2004, he adopted the MNF transformation to remove the noise in image data and got the vegetation fraction by the same linear mixture model[7]. Besides, Tao *et al*. studied the unmixed results after K-L, MNF transformations, and conducted research on the accuracy of SMA, which was of significance[1]. Applications of LSMA to urban land cover and ecological effects are a hotspot in the field of international remote sensing study. It is very important to combine remote sensing with urban geography. However, urban land surface is mainly composed of complicated artificial materials so that the low accuracy of LSMA is the main limitation to its development. Meanwhile, current key problem lies in the selections of endmembers: the range, dimensionality, and the criterion.

According to the Vegetation-Impervious Surface-Soil (V-I-S) conceptual model promoted by Ridd in 1995, urban land cover can be divided into four basic elements: vegetation, high albedo, low albedo, and soil[8]. All pixels in one image can then be interpreted as the combinations of these four elements, which set up a theory foundation for application of pixel unmixture in cities[4,7－9]. As an individual endmember, vegetation plays a distinct role in geography on the basis of the model. Vegetation fraction/abundance was used in many studies to reveal urban green space and its ecological effects. Besides, water was masked from low albedo by some scholars and quantitative model was built combining with high albedo to get urban impervious surface fraction. Similar to vegetation fraction, urban impervious surface influences urban thermal environment and atmospheric condition so it also has distinct effect in geography. However, high albedo and low albedo have not been seriously introduced. This study, based on spectra data measured in field and samples checkup on aerial photograph, finds that low albedo endmember (except water) corresponds to dated buildings in the old city zone while high albedo end-

member corresponds to newly built construction. This phenomenon suggests that changes of high albedo and low albedo endmembers in different periods can represent the spatio-temporal evolvement of urban landscape patterns, especially urban renewal.

Shanghai (Fig. 1), with large amount of shanties where per capita living space is less than 4 m^2 in 1980's, once was the most difficult in project of urban renewal, which is of great value for every municipality to improve civil living conditions and life environment. After two periods' efforts, Shanghai becomes the successful model in urban renewal project[10]. The technique of remote sensing is of significance for detecting the spatial patterns of the old city area renewal. Firstly, the spatial pattern of the urban renewal reveals the changing characters of urban structure and the adjusting direction of urban function, which can provide basic ideas for urban plan in future. Secondly, with the increased urban scale, applying remote sensing to studying urban renewal can supply a low cost but high effective means for programming, implementing and evaluating the renewal engineering. Finally, the study promoted the development of the integration between remote sensing and urban geography. Based on the improved-endmember-selection technology, this paper tries to use LSMA to analyze the spatio-temporal pattern and discuss the application of remote sensing in urban geography from 1997 to 2000.

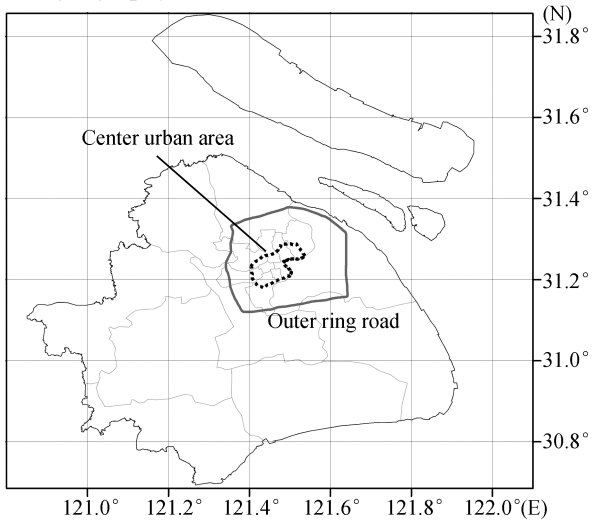

Fig. 1. The geographic map of Shanghai.

1 Method and technology

1.1 LSMA and its improvement

LSMA is a method physically based on image processing, assuming that spectrum measured by a sensor is a linear combination of the spectra of all components within the pixel, and can be expressed as[5]:

$$R_i = \sum_{k=1}^{n} f_k R_{ik} + ER_i, \quad (1)$$

where $i = 1,...,m$ (number of spectral bands); $k = 1,...,n$ (number of endmembers); R_i is the spectral reflectance of band i which contains one or more endmembers; f_k is the proportion of endmember k within the pixel; R_{ik} is the known spectral reflectance of endmember k within the pixel on band i; and ER_i is the error for band i. Root mean square was used to measure the accuracy of solution:

$$RMS = \sqrt{\left(\sum_{i=1}^{m} ER_i^2\right) \Big/ m}, \quad (2)$$

From eq. (2), we can see that the smaller the RMS is, the smaller the error will be.

A constrained inverse least squares deconvolution model was used in this research, assuming that the following two conditions are satisfied simultaneously:

$$\sum_{k=1}^{n} f_k = 1 \quad \text{and} \quad 0 \leqslant f_k \leqslant 1, \quad (3)$$

This will restrict each endmember fraction between 0 and 1; all the summation is equal to 1, which can avoid any fraction larger than 1 or less than 0.

Many studies concluded that the MNF transformation can reduce the correlation between bands and concentrate most information on the first several components, which can improve the accuracy of LSMA as a result[11,12]. According to the analysis above, selecting suitable endmembers is the key factor determining the overall accuracy during the unmixing process. An optimal approach for selecting endmembers is to use laboratory-based measurements of endmember's spectra, referred to as "reference endmember". Although substantial problems exist in correcting atmospheric conditions in satellite sensor data, Gillespie *et al*., Wu *et al*. and others, solved these problems by considering the mixed spectra as a linear combination of endmembers derived from an image (image endmember)[9,13]. Each image endmember is a combination of reference endmembers including atmospheric scattering and absorption[14]. As the spectral information of urban land cover is so complicated, and atmosphere also influences the spectra in addition, image endmember can give a higher accuracy[4−6,9]. Thus, in this study, image

endmembers were chosen and derived from the TM/ETM+ image.

In this paper, to improve the accuracy of LSMA, pixel purity index is introduced to constrict the selection range to very few pure pixels. Besides, we formed a three-dimensional feature space, in which endmember selection interacts with original image, which can also improve the accuracy of results.

(i) Pixel purity index (PPI) The PPI is used to find the most "spectrally pure" or extreme pixels in multispectral and hyperspectral images[15]. Separating purer from more mixed pixels reduces the number of pixels analyzed for endmember determination and makes separation and identification of endmembers easier. The PPI is computed by repeatedly projecting n-dimensional scatter plots onto a random unit vector as shown in Fig. 2. The extreme pixels in each projection are recorded and the total number of times each pixel marked as extreme is noted. In the process of iteration, it asymptotically approaches a flat line (zero slope), which means that all of the extreme pixels have been found. A projection process is performed as follows:

$$dp = \sum_{i=1}^{n} \text{pixel}[i] \cdot \text{skewer}[i], \quad (4)$$

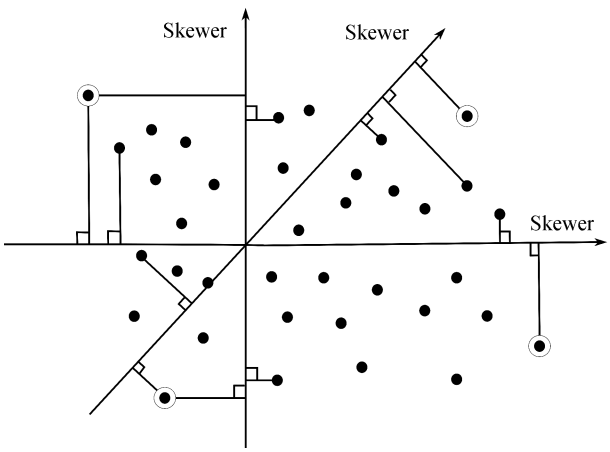

Fig. 2. Schematic view of scatters, which were projected to random skewers in 2D space.

A PPI image is created in which the DN of each pixel corresponds to the number of times that pixel was recorded as extreme. In our study, the number of pixels is 1665292, and when the number of iteration is 10000, the selected pure pixel is 71046 which accounts for 4.26% in all. The number of iteration increases, so does the number of pure pixels selected. When the number of iteration jumps to 15000, the number of pure pixels becomes stable, with 87608 pixels selected, which accounts for 5.26%. A mask gained from the PPI image was used to filter "pure pixels" in which endmembers were selected. Through PPI, the range of selection was reduced by 95%.

(ii) Endmember selection in three-dimensional feature space and unmixing For the components of urban land cover, many studies considered that three or four endmembers can be included, that is, high albedo mainly composed of new building materials such as glass, concrete and light encrust; low albedo including water surface, asphalt, dated roof, etc.; green vegetation such as lawn and woods; soil which in studies of belt between town and country is considered to be the fourth endmember[8]. According to Small's analysis based on the global ETM+ data[5], generally, three typical covers can well depict remote sensing data in urban environment, they are, vegetation, high albedo, low albedo. The paper uses three endmembers for that inside Shanghai City. Fig. 3 depicts the feature space formed by MNF component 1 and MNF component 2. Endmembers "always" present themselves at the corner of triangle. Theoretically, if all of the pixels are within the triangles formed by endmembers, the mixture model can be considered an ideal linear model[9]. The clear delineation of three MNF components (Fig. 4) suggests that the reflectance spectra of the TM or ETM + image might be best represented by a three-endmember linear mixing model.

Traditional method for endmembers selection only considers two dimensions of MNF component 1 and

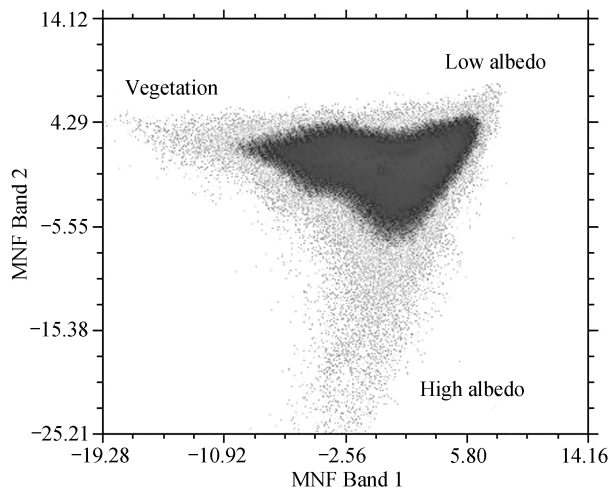

Fig. 3. Pixel scatters plots with a combination of the first two MNF components.

MNF component 2 (Fig. 3)[13,16]. This paper picks out pure pixels by PPI and forms three-dimensional feature space, in which each dot represents a pixel (Fig. 4). The feature space can interact with the original image and the PPI result so that we can see the areal characters and purity. In the selection, we change the angle and direction of coordinate axis, observe pixels polyhedron and its projections on three sides, and check its land cover's purity from PPI and high-resolution aerial photograph. Through continuous filtration, we selected 100 dots for each endmember and the average reflectance of endmembers selected was specified to each ETM+ bands range (Fig. 5).

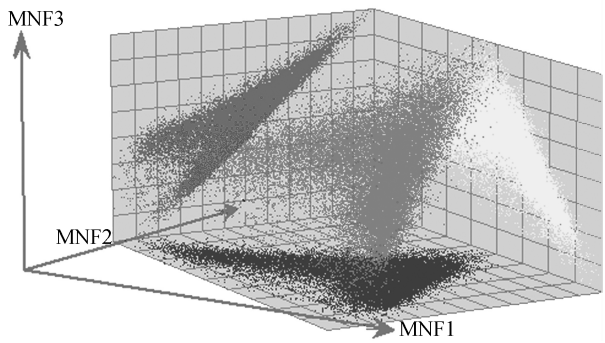

Fig. 4. Pixel scatter plot in 3D space of MNF1－3.

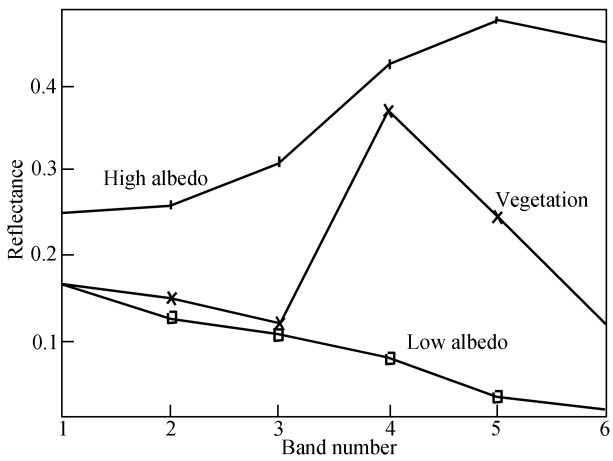

Fig. 5. The reflectance of three endmembers at six bands.

1.2 Checkup of the land surface characteristics of high and low albedo endmembers

(i) Spectrum reflectivity checkup by spectrometer

There are still general rules for complicated urban land cover. To reveal reflectance spectral features of urban landscape, we measured the spectrum reflectivity on the spot of several typical urban building surfaces by spectrometer. The number of measured points is 171 while the number of spectrum is 2305. Three types of urban building surfaces can be classified: roads, rooftops and soil which in summer is too little in central city to consider. The spectrum reflectivity of glass or metal overlaying on high buildings and large mansions preponderates over the range of spectrometer. New buildings are often covered by concrete whose spectrum reflectivity is higher than 35% between 400 and 900nm, much higher than old cement surface, roof and asphalt surface. For old city zone in Shanghai, the main building surface cyan-tiled roof's spectrum reflectivity is obviously lower than old cement surface[1]. In addition, asphalted rooftops and roads surface which has low spectrum reflectivity were adopted in the past instead of concrete, building decorative materials, glass, metal and green vegetation now. So we conclude that the evolvement of high albedo and low albedo can reflect urban renewal and sprawl.

Furthermore, from Fig. 6 we can see that there lies contrary trend between actual spectrum of old construction surface and the results of low albedo in Fig. 5 derived from LSMA, for the unmixed image without atmosphere correction, which was caused by the following two reasons: the air path radiation (including Rayleigh scatter and Mie scatter) caused by grains in atmosphere will be cut down with the increase of wavelength; generally, steam in atmosphere has higher absorption to the radiation in infrared band than in visible band. But all these would produce little influence on the result using high or low albedo to represent new or old building.

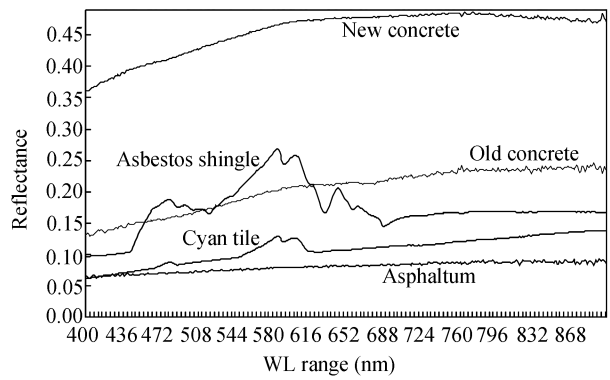

Fig. 6. The spectrum reflectivity on the spot of several typical urban building surfaces.

1) Xu, L. H., Air path radiation and atmospheric quality of Shanghai, Thesis for doctor degree of East China Normal University, 2005.

(ii) High-resolution measurement of high albedo fraction To reveal the relationship between the newly-built area and high albedo, we selected 75 samples randomly in aerial colorful photograph. Screen digitization was conducted to specify new buildings. Comparing these samples with values of high albedo endmember fraction from LSMA, we found a good consistency between them (Fig. 7). But there are several problems: temporal differences, new building judgment, and digitization error, but the consistency is so obvious that the mean error between both is only 0.044. So we conclude that high albedo endmember can represent new buildings.

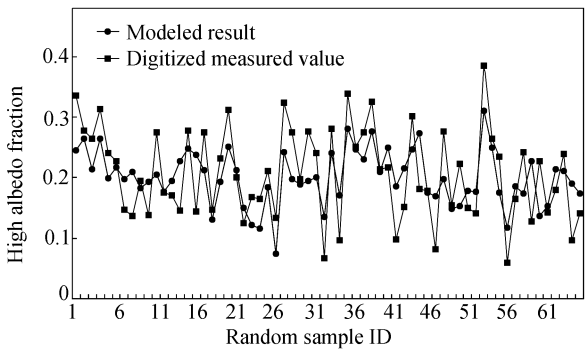

Fig. 7. Comparison of high albedo fraction between digitized and modeled.

1.3 Validation

(i) Root mean square (RMS) During the process of "unmixing", errors from the data preparation, endmembers selection and the linear mixing model by least squares will reduce the accuracy of vegetation fraction[7]. The RMS for every image pixel was calculated in order to assess the performance of this moedl. According to formula (2), obviously, the lower the RMS is, the better fit the model will be. Every pixel's RMS of 2000 is shown as Fig. 8. The maximal value is 0.0867 and most are lower than 0.01 according to RMS frequency histogram. 98.5% of RMS is smaller than 0.02, which shows a better result than the former studies[4]. But the distribution of RMS is not symmetrical. As a whole, the values located in urban area are higher than in suburb, and in the old city area are also higher than in newly-built city area. Comparatively, mixed pixels are more inclined to have large RMS than pure pixels. The more complicated the inside mixed pixel is, the large the RMS will be, which suggests there may be another spectral endmember to be further studied.

(ii) Accuracy assessment According to LSMA theory above, the relationship between the three endmembers is linear, and the total fraction should be equal to 1 in a unit pixel. So, if we can determine the accurate fraction of one or two endmembers, the accuracy of results is relatively high on the whole. In the urban central area, impervious surface can be considered as summation of high albedo and low albedo except for water[9]. We digitized impervious surface fraction on aerial photograph within random square samples (masked off water) and got statistical results of LSMA. As a result, we had a digitized impervious surface fraction (actual fraction) and statistical impervious surface fraction (modeled fraction). Comparison is made between them for rigorous purpose.

In order to assess accuracy of impervious surfaces estimation, a random sampling method was applied. We randomly selected 127 rectangular windows with 150m×150m in color aerial photograph based on the principle that each window should contain some urban

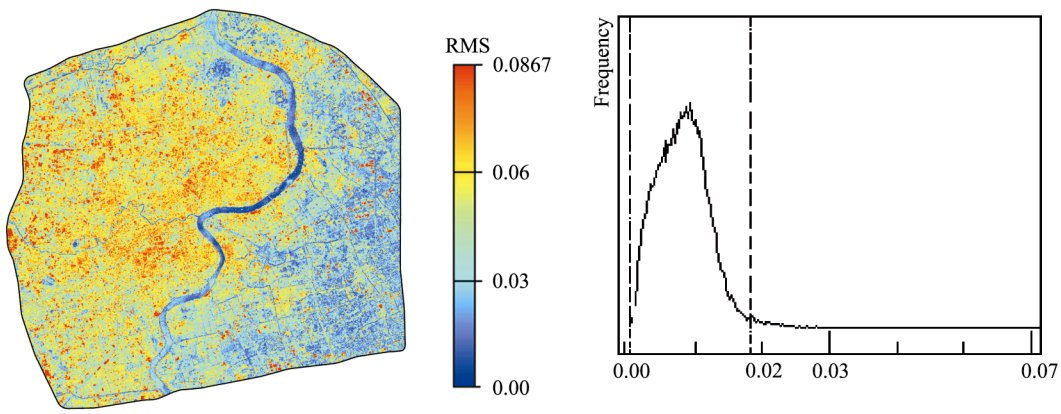

Fig. 8. The image and frequency plot of root mean square.

buildings. We then digitalized the impervious surface manually in the 127 windows, whose actual abundance then can be obtained. These windows were then used to extract the sum of high and low albedo above and got the results of LSMA with the above models. Fig. 9 shows the comparison of the two results and the residual. Except for some windows with the residual higher than 0.4, most were within ± 0.2 and decreased as the abundance of impervious surface increased. The accuracy was evidently increased compared to the similar researches[9].

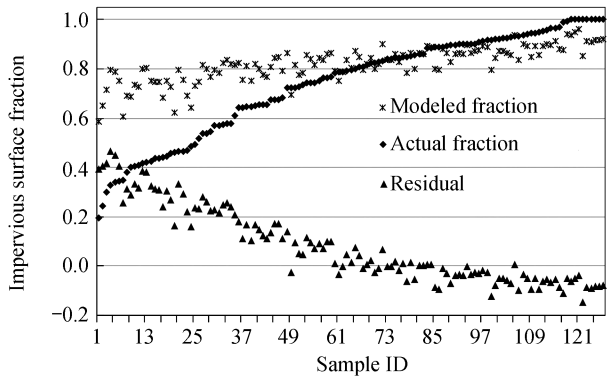

Fig. 9. Accuracy assessment result of impervious surface estimation.

2 Results and analysis

2.1 The results of LSMA

According to discussion above, the LSMA results of 1997 and 2000 are shown as Figs. 10 and 11. Shanghai City was in the stage of rapid expanding and changing between 1997 and 2000. Many buildings were built with the materials such as metal, concrete and glass with high reflectivity. It is obvious that there is a great difference between urban and suburb based on the fraction image of high albedo. In the brim of urban, high values appear less than the central area in high albedo fraction imagery except for a few old towns. In addition, the distribution of high albedo fraction inside urban area focuses on newly built urban areas mainly at the frontier of urban sprawling and residents in renewal areas. However, low albedo, representing land covers such as water, old buildings and heavy industry areas seriously polluted for quite a few dusts, most shows low values except the following areas, old urban area between the People Square and the bund along with both sides of Suzhou River, and Wusongkou area giving priority to industry land, which have rather higher values. The main characters of urban evolvement is that with the old city area's renewal and urban sprawl, in the central city area many old buildings showing low albedo are replaced by vegetation and new buildings having high albedo. While in suburb, farmland paddies were transformed to new buildings (high albedo). With the importance of urban ecological environment emerging, vegetation abundance inside city is obviously increasing especially newly-built park and large lawn. Vegetation fraction reached to 60% above in New Jiangwan Town, Youthful Forest Park, Lujiazui Park and Changfen Park in 2000.

2.2 The pattern and mode of urban renewal in center urban area (1997—2000)

According to the analysis above, we drew the conclusion that LSMA with improved endmember selection had relatively high accuracy. Two ways of spectral test and sample-in-field test proved that the abundance of high and low albedo could reflect different characters of the construction surface. Therefore, the changes during different periods could be used to analyze the

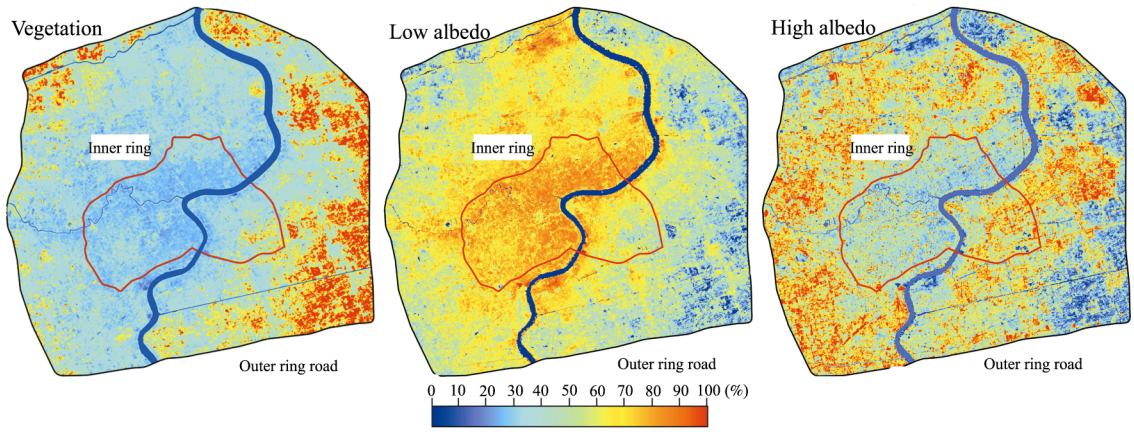

Fig. 10. Three-component endmember fraction images of Shanghai City in 1997.

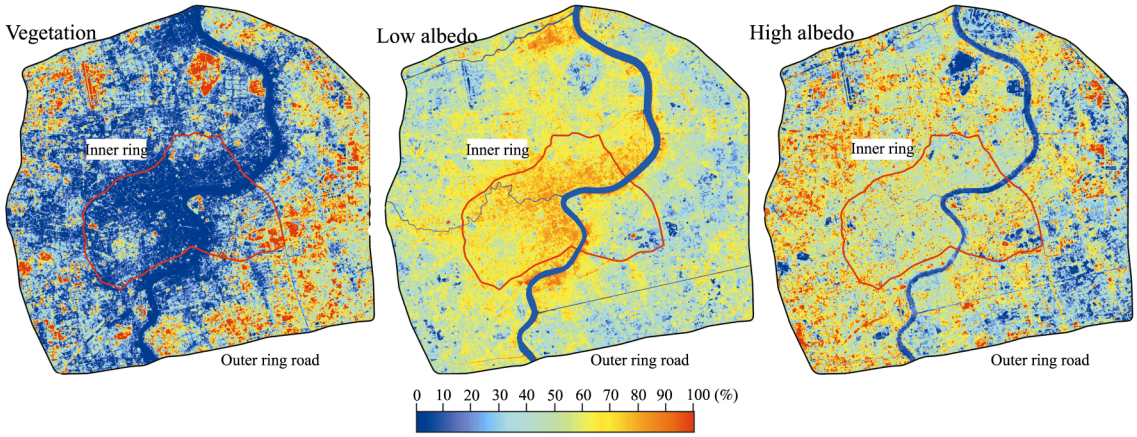

Fig. 11. Three-component endmember fraction images of Shanghai City in 2000.

urban sprawl and the renewal of the old city area. This paper selects two TM/ETM+ images of 1997 and 2000 for the urban renewal analysis. Since this period was just when Shanghai underwent the first round urban renewal, this paper focuses on the old city area which is on the west of Huangpu River inside the inner ring road and discusses the pattern and mode of the urban renewal.

If the low albedo fraction in one pixel increases significantly, we can think that urban renewal is conducted in the pixel because water varies little in temporal images while old buildings then influence the fraction obviously. Considering that one pixel is represented by three components, we chose 15% fraction as a threshold. Within one pixel, if the increase of low albedo fraction goes over15%, we regard that urban renewal happened similarly, the evolvement of vegetation and high albedo is judged by the same principle. If the increase of vegetation fraction goes over 15%, we regard that the city renewal happened, that is, the green vegetation replaced old buildings. If the increase of high albedo fraction goes over 15%, we regard that the city renewal happened; new buildings played a prevailing role. If the increase of high albedo fraction and vegetation fraction goes less than 15%, we regard that the city renewal happened; new buildings and vegetation were both conducted. Fig. 12 shows us the pattern and mode of the urban renewal between 1997 and 2000 by the way of raster calculation supported by ARCGIS/GRID. In Fig. 12, red, green and blue colors represent renewal areas of urban renewal. Red color refers to new buildings; green color refers to vegetation; blue color refers to both new buildings and vegetation.

From the result, we found that the main renewal areas were changing from CBD in central urban (between

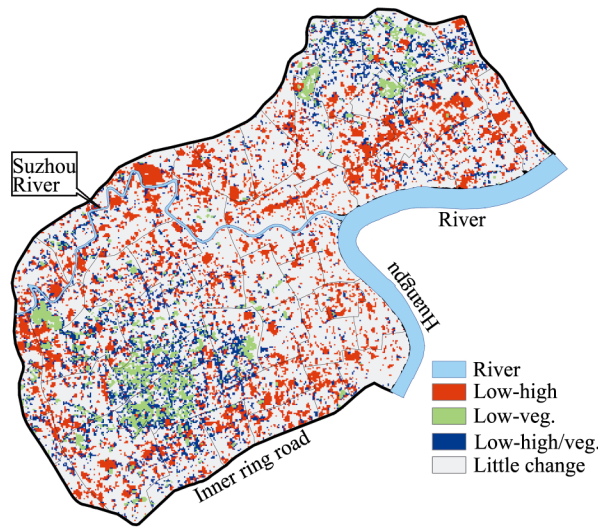

Fig. 12. The pattern and mode of urban renewal at pixel scale from 1997 to 2000.

Nanjing Road and Huaihai Road and around Yuyuan Park) to the inner ring road. Besides Yangpu District and part of Hongkou District near Huangpu River, other areas which were mainly rebuilt with new construction distributed in Putuo District, Changning District, Xuhui District and part of Luwan District near inner ring road. Another characteristic in this urban-renewal was the recovery of vegetation and the constructing of large parks. There were two districts with greatly increased vegetation: one was the communities of Hunan Road and Tianping Road on the north of Xuhui District. These areas used to be French settlement and the main construction was villas in old style. In the recent years, more trees were planted among these villas resulting in the increased abundance of vegetation. Other areas were large greenlands in Hongkou District, Changning District and the north of

Luwan District, e.g. the large green land in Tianshan Park where Yan'an Elevated Road and inner ring road met, Luxun Park and Heping Park etc. Between CBD and those areas above, most old residential areas were reconstructed to new residential administration areas. The reconstruction of these areas included increasing both new construction and vegetation to reduce the building density and increase the abundance of vegetation.

The first round urban renewal of Shanghai City (1992－2000), "365 Urban Renewal Project", was to reconstruct the old building with areas of 3.65×10^6 m^2. Statistically, 3.8×10^7 m^2 of old city areas was reconstructed including more than 4×10^6 m^2 of risky houses and 1×10^6 residents moved to new houses. Between 1995 and 2000, about 3×10^7m^2 of aged construction was removed[1]. According to the result of LSMA, between 1997 and 2000, 19.93% areas of urban renewal inside inner ring road on the west of Huangpu River were 1.576×10^7 m^2 and took up nearly half of the total areas of reconstruction; 7.9×10^6 m^2 new buildings were reconstructed and took up 50.13% of urban renewal; the renewal of vegetation recovery and greenland constructing was about 2.72×10^6 m^2 and took up 17.26% of the total renewal area; The reconstruction of both took up 32.61%. Thus it can be seen that the scale of urban renewal is very big. The renewal of residential and administration area is the mainstream accompanied by

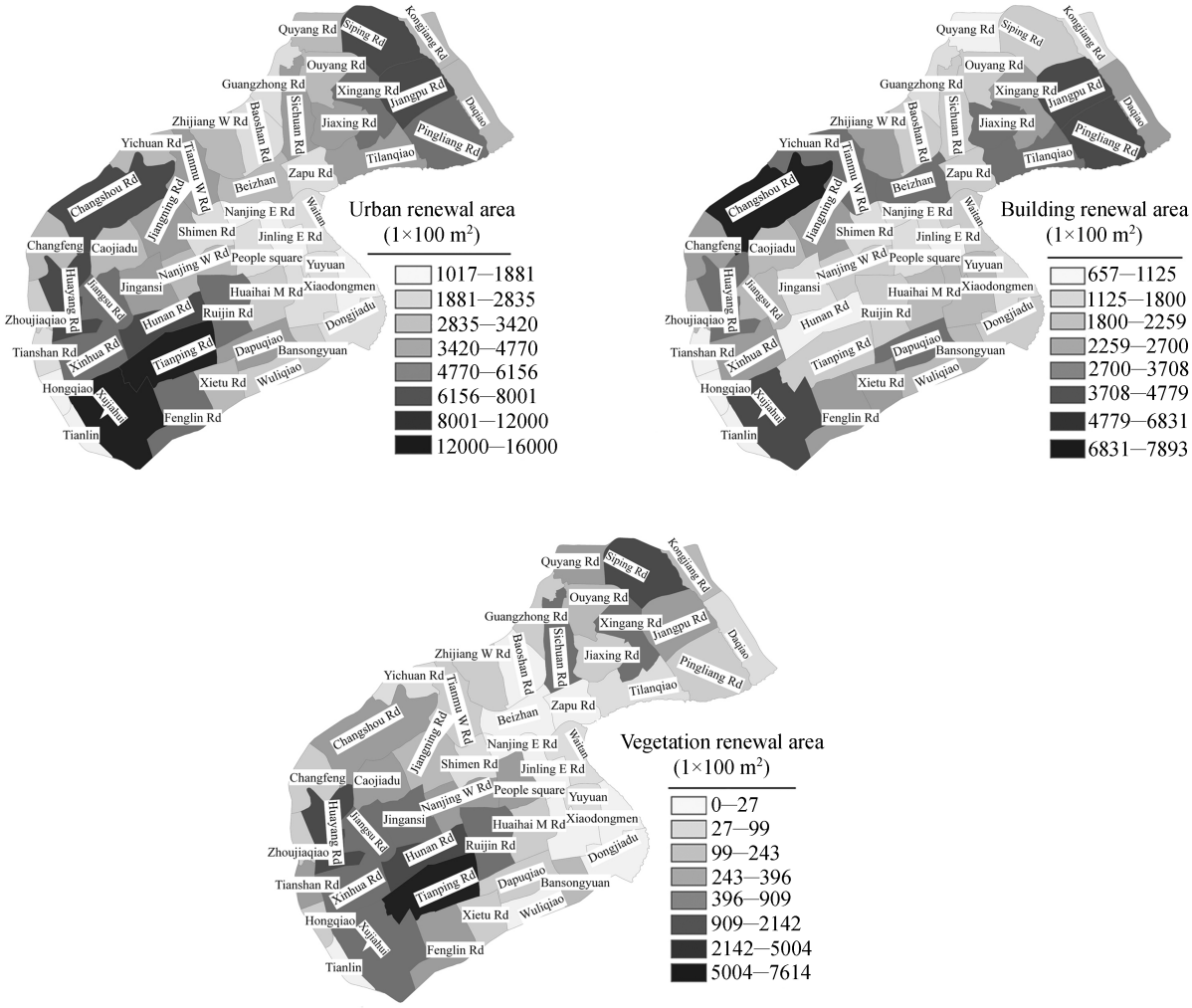

Fig. 13. The pattern of urban renewal on street community scale.

1) Wang, W., Fu, G. L., It is perfect for urban renewal in Shanghai, Wen Hui Daily (in Chinese), July 17, 2003.

cosmically-built infrastructure. Inner Ring Road, Yan'an Elevated Road, North-South Elevated Road, subway line No.1 and No.2 and elevated road No. 3 have been built or are being built. Green vegetation cover is more and more increasing for its importance to urban environment. Results from LSMA accord with statistical data to some degree except temporal difference that one image is photoed in April, 1997 and the other is in June, 2000, which leads to the vegetation fraction in 2000 much higher than that in 1997.

2.3 The pattern and mode of urban renewal at the street community scale

We analyzed the urban-renewal results above at the pixel scale. Due to the low resolution at the pixel scale, areas of urban-renewal and its trend were distributed to each community to further analyze the spatial pattern and its characters in detail from 1997 to 2000.

On the community scale (Fig. 13), spatial pattern of urban-renewal from 1997 to 2000 was more obvious. Most evident areas spread out along inner ring road including street communities of Siping Road, Jiangpu Road and Pingliang Road in Yangpu District, Xingang Road in Hongkou District, Changshou Road in Putuo District, Huayang Road and Xinhua Road in Changning District, Xujiahui, Hunan Road and Tianping Road in Xuhui District from north to south, while the core areas to the east of People Square are lightly renewal. The most renewed communities were Xujiahui Road and Tianping Road in Xuhui District. When coming to the renewal patterns, Jiangpu Road and Pingliang Road in Yangpu District in the north, Changshou Road in Putuo District in the west, and Xujiahui Road in Xuhui District and Dapuqiao Road in Luwan District in the south were mainly changed by newly-built construction and formed a semi-circularity facing to the east. The areas most changed by vegetation included: Siping Road in the north, Tianping Road, Hunan Road and Huayang Road in the South and formed two highly centralized areas in south and north. Among them, the most greatly changed areas were where Xuhui, Jing'an, Changning and Luwan Districts matched, while for the high land value in the middle areas along Suzhou River and in the east of Huangpu District, the vegetation fraction increased little[17,18]. On the periphery mainly covered with vegetation, the newly-built vegetation on the prevenient basis had led to relatively high vegetation abundance; there was rarely newly-built vegetation among old construction and most of them were distributed around the crossroads; the vegetation among newly-built residential construction was mainly small patches but had a broad distribution, which contributed to the improvement of ecological environment in center of the city.

3 Conclusions and discussion

This paper, based on the Landsat TM/ETM+ imagery, uses improved LSMA and discusses the method and significance of the urban renewal in the field of remote sensing. The conclusions and discussion were shown as follows:

(1) Aiming at the restricted factors in LSMA, PPI was introduced to help to select endmembers and reduce the extent of endmember selection by 95%. The first three MNF components are selected to form three-dimensional mixing space. By expanding the traditional two-dimensional mixing space to three-dimensional mixing space, the third component is considered, and during the process, we compared the original and high-resolution imagery with the results of PPI, which will obtain more accurate results.

(2) Spatio-temporal changing of high and low albedo and endmembers of vegetation was used to reflect the pattern of urban-renewal, which provides a new way to study the urban landscape changing in the field of urban geography. The precondition of this idea is based on the strict spectral test and field test. With the test of spectral reflectivity in field and random-chosen samples in high resolution color aerial photograph, the pattern and mode of urban-renewal can be explained by the changing abundance of high and low albedo.

(3) The quantitative calculation of LSMA of the period reveals the pattern of urban renewal. At the scale of pixel, the focus of urban renewal is extended from CBD to the inner ring road and forms a region of semi-circularity; the main mode of renewal was the change from old construction to new construction accompanied by recovered and newly built vegetation; nearly 1/3 of the newly built construction was residential and administration area with reduction of building density and increase of vegetation. When coming to the scale of street community, the communities of Siping Road, Jiangpu Road, Changshou Road, Xujiahui Road and Tianping Road show the most obvious changing; light reconstruction was detected along the Suzhou River and Huangpu District; newly built construction took up most on the northeast, west and southwest of the region while Tianping Road and Siping Road were

mainly reconstructed by the cover of vegetation.

(4) Although comparing to the current research, accuracy of LSMA is increased by the improvement of endmember selection, in essence, evaluating the quantity and quality of endmembers directly from image still is lack of quantitative criterion. Besides, the complex landscape of urban and temporal difference of imagery, some low albedo still can be detected in the newly built construction and that may lead to some errors in the results, e.g. over increased abundance of vegetation due to the temporal difference of imagery. Confirmation of criterion of endmember evaluation, application of automatic selection by computer and finding the typical objects with different reflectivity in both old and new construction by spectral analysis all need to be further studied.

Acknowledgements The authors would like to thank Editor Li Yawen, Prof. Wei Ji and two anonymous referees for their valuable comments on an earlier draft and pains for revising the paper, and especially Prof. Wei Ji and the two referees who gave much important suggestion to the paper. This work was supported by the National Natural Science Foundation of China (Grant No. 40371092).

References

1 Tao Q X, Tao H X, Zhang L P. Study on applying linear mixing spectral model in vegetation classification using hyperspectral remote sensing. Survey Technology (in Chinese), 2004, (1): 21－24

2 Shimabukuro Y E, Smith J A. Least squares mixing models to generate fraction images derived from remote sensing multispectral data. IEEE Transactions on Geoscience and Remote Sensing, 1991, 29: 16－20

3 Emma U, Susan U, Deanne D. Mapping nonnative plants using hyperspectral imagery. Remote Sensing of Environment, 2003, 86: 150－161

4 Small C. Estimation of urban vegetation abundance by spectral mixture analysis. International Journal of Remote Sensing, 2001, 22(7): 1305－1334

5 Small C. Multitemporal analysis of urban reflectance. Remote Sensing of Environment, 2002, 81: 427－442

6 Lü C C, Wang Z W, Qian S M. A review of pixel unmixing model, Remote Sensing Information (in Chinese), 2003, 3: 55－60

7 Small C. The Landsat ETM+ spectral mixing space. Remote Sensing of Environment, 2004, 93: 1－17

8 Ridd M K. Exploring a V-I-S (vegetation-impervious surface-soil) model for urban ecosystem analysis through remote sensing: comparative anatomy for cities. International Journal of Remote Sensing, 1995, 16: 2165－2185

9 Wu C S. Estimating impervious surface distribution by spectral mixture analysis. Remote Sensing of Environment, 2003, 84: 493－505

10 Yao K. The diagnosis for Shanghai urban renewal. Beijing Plan and Construct (in Chinese), 2004, 1: 151－153

11 Ma J W, Zhao Z M. Buheaosier, Remote Sensing Data Model and Processing Method (in Chinese). Beijing: Chinese Science and Technology Press, 2001, 62－70

12 Smith M O, Johnson P E, Adams J B. Quantitative determination of mineral types and abundances from reflectance spectra using principal components analysis. Journal of Geophysical Research, 1985, 90: 797－804

13 Gillespie A R, Smith M O, Adams J B, et al. Interpretation of residual images: spectral mixture analysis of AVIRIS. In: Proceedings of the 2nd AVIRIS workshop, 4－5 June 1990 (Pasadena, CA: JPL): 243－270

14 Van Der Meer F, De Jong S M. Improving the results of spectral unmixing of Landsat Thematic Mapper imagery by enhancing the orthogonality of end-members. International Journal of Remote Sensing, 2000, 21: 2781－2797

15 Boardman J W, Kruse F A, Green R O. Mapping target signatures via partial unmixing of AVIRIS data. In: Summaries, Fifth JPL Airborne Earth Science Workshop. JPL Publication 95-1, 1995,1: 23－26

16 Weng Q, Lu D, Schubring J. Estimation of land surface temperature-vegetation abundance relationship for urban heat island studies. Remote Sensing of Environment, 2004, 89: 467－483

17 Xu J H, Yue W Z, Tan W Q. Spatial stat. law for the effect of urban sight structure. Acta Geographica Sinica (in Chinese), 2004, 59(6): 1058－1065

18 Yue W Z, Xu J H, Tan W Q. Spatial scale analysis of the diversities of urban landscape. Acta Ecologica Sinica (in Chinese), 2005, 25(1): 122－128

(Received September 23, 2005; accepted November 7, 2005)